Alternative Venous Pathways: A Potential Key Imaging Feature for Early Diagnosis of Sturge-Weber Syndrome Type 1

Carmen R. Cerron-Vela, Amirreza Manteghinejad, Simon M Clifford and Savvas Andronikou

ABSTRACT

BACKGROUND AND PURPOSE: Sturge-Weber syndrome is a rare congenital disorder characterized by cortical atrophy and calcifications on late-stage imaging. Understanding the evolution of brain lesions is crucial for effective early interventions, yet the timeline remains unclear. We aimed to evaluate early brain MRI findings and their progression longitudinally on follow-up MRI in children diagnosed with Sturge-Weber syndrome.

MATERIALS AND METHODS: We retrospectively included all children with a confirmed diagnosis of Sturge-Weber syndrome between 2009 and 2023 that had at least 2 available MRIs performed before the age of 2 years. A pediatric radiologist and a pediatric neuroradiologist evaluated all the MRI scans for pial enhancement, choroid plexus enlargement, atrophy, calcifications, a prominent subarachnoid varicose network, trans medullary veins, subependymal veins, and deep extra ventricular veins. Descriptive analysis was used for demographic data and brain lesion prevalence. Cumulative incidence curves were used to show the timeline of emerging lesions. K-means clustering was used to categorize the lesions based on their prevalence at 1, 2, 3, 6, 12, 18, and 24 months after birth.

RESULTS: Nine patients met the inclusion criteria. Median ages at the first and last MRIs were 35 days (IQR: 11-123) and 294 days (IQR: 208-465), respectively. The most prevalent lesions at the first MRI were subarachnoid varicose network (88.9%) and trans medullary veins (77.8%), while prevalence of atrophy and calcifications differed most between the first and last MRIs. The results of the elbow method and K-means clustering showed that we can divide Sturge-Weber syndrome lesions into 3 groups based on their timeline of emergence. The first cluster contained subarachnoid varicose network, trans medullary veins, subependymal veins, and choroid plexus enlargement. The second cluster contained deep extra ventricular veins, pial enhancement, accelerated myelination, and atrophy. The last cluster contained calcifications.

CONCLUSIONS: Our findings suggest that dilated venous channels emerge early as a compensatory mechanism, preceding atrophy and calcification. Additionally, these dilated channels precede the appearance of abnormal contrast enhancement of the pia, often termed leptomeningeal angioma. This underscores the importance of early recognition and monitoring of these initial imaging indicators in clinical practice.

ABBREVIATIONS: ASL = Arterial Spin Labelled; MinIP = Minimum intensity projection; SWS = Sturge-Weber Syndrome

SUMMARY SECTION

PREVIOUS LITERATURE: In Sturge-Weber syndrome (SWS), abnormal cortical venous drainage results in deep venous collaterals. Failure of compensatory venous drainage causes venous congestion, hypo-perfusion, chronic anoxia, neuronal gliosis with eventual atrophy and cortical calcification. Traditionally pial enhancement is the key diagnostic imaging sign of SWS - the so-called "pial angioma." In addition to enhancement of the pia, a network of varying-sized venous structures with flow-voids is seen separately in the subarachnoid space.

KEY FINDINGS: Pial enhancement itself is not as frequently present in the very early stages of SWS (although it can be seen within the first 2 months), and is preceded by the appearance of centripetal venous drainage compensatory pathways and the subarachnoid varicose network, likely a centrifugal alternative pathway.

KNOWLEDGE ADVANCEMENT: For children with high-risk port wine stain, early imaging, before 3 months of age, should include T2 and MinIP SWI sequences to identify alternative venous pathways. This includes detection of the subarachnoid varicose network, seen separate from pial enhancement, visualized without and with contrast enhancement.

INTRODUCTION

Sturge–Weber syndrome (SWS) is a rare congenital disorder characterized by cutaneous, neurological, and ocular manifestations due to capillary-venous malformations in the skin, brain, and eye, caused by a somatic mutation (p.Arg183Gln, p.R183Q) in the guanine nucleotide-binding protein G(q) subunit alpha (GNAQ) gene. In the brain, SWS is characterized by the development of what has been termed, even recently, as a leptomeningeal or pial "angioma," leading to chronic brain injury [1].

Abnormal cortical venous drainage and abnormal deep venous collaterals are implicated in the pathophysiology of intracranial abnormalities in patients with SWS [2]. These abnormalities lead to cerebral parenchymal venous congestion, later resulting in hypo-perfusion, chronic anoxia, neuronal gliosis, atrophy, and cortical calcifications [3], the imaging corollary of which has recently been demonstrated using perfusion (arterial spin labeled) MRI [4]. SWS therefore presents as an evolution of imaging findings that may include abnormal venous structures, development and evolution of venous compensatory pathways, signs of venous congestion, hypoperfusion, and parenchymal necrosis with eventual development of the classic SWS features of atrophy and calcification.

Most patients with brain involvement will begin seizure activity by 2 years of age [5], which is a landmark in the progression of SWS. The so-called *pre-symptomatic phase* constitutes a critical time window for treatment or intervention that may delay or even avoid seizures with subsequent improvement of neurological outcomes [6]. Although some studies have investigated early MRI features to diagnose brain involvement in the pre-symptomatic phase [7–10], SWS disease progression and, therefore, the progression of imaging findings remain unclear.

Many authors agree that when screening infants with high-risk SWS, negative MRI cannot be considered conclusive if performed early. Still, there is no consensus regarding who to screen or the age at which a negative scan can reliably exclude SWS [11,12]. We aimed to evaluate the evolution of brain changes in children with SWS on brain MRI that occur before 2 years of age and establish a possible timeline of venous and parenchymal changes that may guide the early assessment and management of these patients.

MATERIALS AND METHODS

We conducted a single-center, retrospective study in a large tertiary pediatric hospital. Our study was reviewed and approved by our institutional review board and complied with the Health Insurance Portability and Accountability Act. We obtained a waiver for documentation of informed consent.

From our clinical radiology database, we retrospectively identified all patients with suspected clinical diagnoses of SWS, later confirmed with imaging, between 2009 and 2023 using mPower (by Nuance Communications Inc., Burlington, MA) and Illuminate (InSight, Overland Park, KA). We obtained demographic and clinical data from an electronic chart system (Epic Systems Corp., Verona, WI). The inclusion criteria were as follows: patients with a confirmed clinical diagnosis of SWS with at least 2 available MRIs before the age of 2 with a gap of at least 2 months between scans. (Online Supplemental data)

Imaging data acquisition

All patients underwent either 1.5 or 3.0 Tesla brain MRI (Siemens Medical Solutions, Erlangen, Germany). Slice thickness varied from 2 to 4 mm with an interslice gap from 0 to 3 mm. Sequences performed included at minimum T1WI, T2WI, T2-FLAIR, and Gadolinium-enhanced T1WI TSE (Gad TSE T1WI). Depending on the scanner, SWI and ASL perfusion sequences were also available on most MRI scans.

Image analysis

All imaging was retrospectively reviewed in consensus by a pediatric radiologist (with four years of experience) and a pediatric neuroradiologist (with more than 20 years of experience). The following parameters were recorded (according to MR sequence):

T2WI

- Brain hemisphere involvement (unilateral, bilateral)
- Cortical atrophy
- Venous abnormalities (including choroid plexus thickening)
- Myelination changes

Minimum intensity projection (MinIP) SWI

- Venous abnormalities
- Presence of calcifications

Gad TSE T1WI

- Pial enhancement

ASL

- Perfusion

59   Vein abnormalities were categorized based on their anatomical distribution into the following [3,13-15] (**Figure 1**):

60   *Subarachnoid varicose network:* We
61   developed this term to describe what has
62   previously been (likely erroneously) termed a
63   *leptomeningeal* or *pial angioma,* which has been
64   used to describe the engorged pial vessels with
65   corresponding thickening of the leptomeninges
66   and post-contrast-enhancement, secondary to the
67   abnormal cortical venous drainage [3,16,17]. The
68   subarachnoid varicose network represents an
69   engorged venous plexus over the cerebral surface
70   which likely drains through developmental venous
71   anomaly-like channels and hypertrophy of a small
72   group of remnant trans cerebral veins toward the
73   subependymal vessels only, without any
74   superficial drainage [3,14].

75   *Trans medullary veins:* composed of the deep
76   medullary veins, responsible for the deep drainage
77   of the white matter as they traverse the white
78   matter to connect with subependymal veins.

79   *Subependymal veins or periventricular veins:*
80   veins that receive blood from the deep medullary
81   veins and subsequently drain into the larger
82   internal cerebral veins.

83   *Deep extra ventricular veins:* vein tributaries
84   to the internal cerebral veins, including the direct
85   lateral and medial atrial veins, and tributaries to the
86   basal vein of Rosenthal, including the deep middle
87   cerebral vein and inferior ventricular vein, which
88   eventually join the vein of Galen and then drain to
89   the straight sinus [15]

90   *Data Analysis:*

91   We used descriptive statistics for demographics.
92   The prevalence of brain lesions was presented as
93   frequencies and percentages. A spider plot was
94   also used to show the prevalence of brain lesions
95   at the first and last MRIs. To show the trend of
96   developing lesions, cumulative incidence curves
97   were used. Log-rank tests were used to compare
98   the trends of developing lesions. Finally, we used K-means clustering to categorize brain lesions based on their time of
99   development. To achieve this, we generated variables representing the prevalence of each lesion at specific time points: 1 month,
100   2 months, 3 months, 6 months, 12 months, 18 months, and 24 months after birth. We also used the elbow method to find the
101   optimum number of clusters.
102   SPSS Statistics (version 29.0; IBM Corp., Armonk, NY) and scikit-learn (version 0.23.2) [18] library were used to analyze the
103   data. A p-value < 0.05 was used to indicate statistical significance. Plots were created using Seaborn (version 0.11.2) and Matplotlib
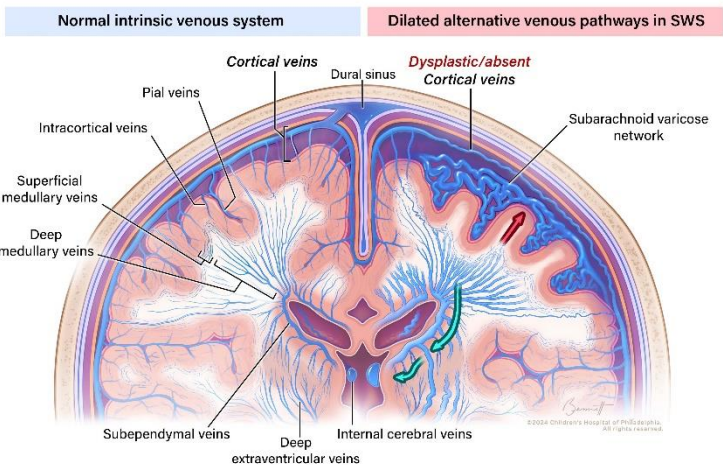104   (version 3.5.2) libraries in Python.

105

Figure 1. Coronal illustration of bilateral brain hemispheres depicting the organization of the normal intrinsic venous system and the development of dilated alternative venous pathways in Sturge Weber Syndrome (SWS).

Normal intrinsic venous system: The superficial cerebral venous system comprises cortical veins, superficial medullary veins, and smaller vessels such as intracortical veins and pial veins. These vessels ultimately drain into the dural venous sinuses. The deep cerebral venous system consists of the deep medullary veins, which converge towards the ventricles and merge with the subependymal veins, eventually draining into the internal cerebral veins. Other veins contributing to the internal cerebral veins are referred to as deep extra-ventricular veins. The paired internal cerebral veins later drain into the vein of Galen.

Dilated alternative venous pathways in SWS: In areas of the brain affected by SWS, the absence or dysplastic cortical veins leads to abnormal drainage of the superficial venous system with redirection of flow towards the deep venous system (green arrows), resulting in secondary engorgement of deep medullary veins, subependymal veins, and deep extra ventricular veins; as well as centrifugal rerouting into the subarachnoid varicose network (red arrows).

RESULTS

Nine children, comprising 5 (56%) boys and 4 (44%) girls, formed part of this study based on the inclusion and exclusion criteria. Five (56%) children had 2 MRIs before the age of 24 months, while the other four (44%) had 3 MRIs. The median age at the time of the first MRI was 35 (IQR:11-123) days and at the last MRI 294 (IQR: 208-465) days.

The most common brain findings overall throughout the whole cohort were prominent deep extra ventricular veins, pial enhancement, and atrophy, which were seen in all the patients.

Comparing the first and last MRIs, findings of a prominent subarachnoid varicose network and trans medullary veins had the highest prevalence (88.9% and 77.8%, respectively) at the time of the first MRI, while atrophy and calcifications had the highest prevalence difference between the first and last MRI. **Figure 2** demonstrates the prevalence of each finding in the first and last MRIs. Detailed individual patient MRI findings are summarized in Online Supplemental data.

The cumulative incidence curves in **Figure 3** show the timelines of visualization of the

Figure 2. Spider (radar) plot showing the temporal in the prevalence of brain lesions from baseline MRI (blue) to the last brain MRI (red). Each spoke represents a lesion prevalence. The distance from the center to a point on a spoke indicates the prevalence percentage for that category.

subarachnoid varicose network, trans medullary veins, subependymal veins, and deep extra ventricular veins against pial enhancement in the first 2 months of life and against calcifications in the first 24 months of life. During the first 2 months, although the difference was not significant, the subarachnoid varicose network, trans medullary veins, subependymal veins, and deep extra ventricular veins tended to appear earlier than pial enhancement. During the first 24 months, there is a significant difference in the timing of visualization of the subarachnoid varicose network with the appearance of calcifications (p<0.001), noting that calcifications occur later in the progression of the disease.

Online Supplemental Data shows the elbow plot for finding the best number of clusters, from which we chose to have 3 clusters. The results of K-means clustering showed that the first cluster contained subarachnoid varicose network, trans medullary veins, subependymal veins, and choroid plexus enlargement. The second cluster contained deep extra ventricular veins, pial enhancement, accelerated myelination, and atrophy. Finally, the last cluster contained calcifications.
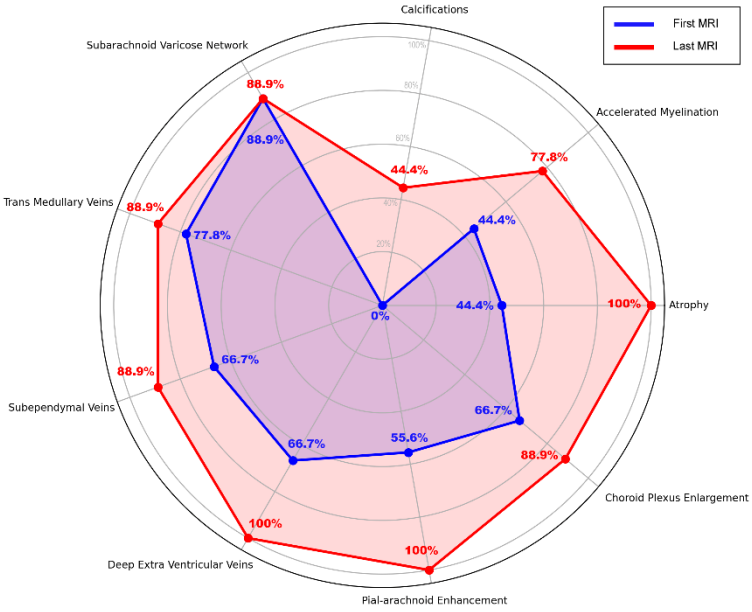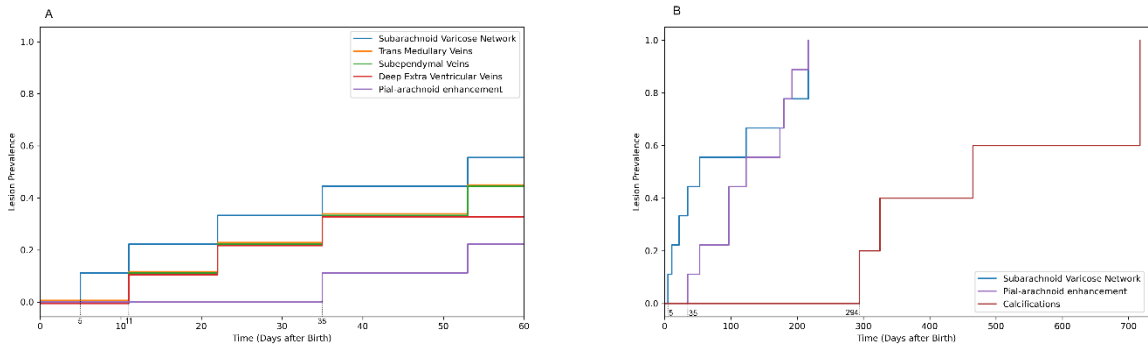

Figure 3. (a) Cumulative incidence curves comparing the timeline of involvement of cerebral venous structures based on the age of patients (days) in the first 60 days. (b) Cumulative incidence curves comparing the timeline of calcifications, pial enhancement, and subarachnoid varicose network in the first 2 years.

DISCUSSION

In this study, we evaluated early brain MRI findings in a series of 9 patients with the diagnosis of SWS from imaging performed while the patients were under 2 years of age and demonstrated important differences in the timing of the appearance of different imaging findings.

In SWS, the classically described imaging findings using MRI or CT are superficial cerebral calcification, atrophy, and leptomeningeal enhancement [19]. However, our findings show that these observations do not manifest in the early phases of the disease and represent eventual outcomes of overburdened compensatory mechanisms resulting in cortical and subcortical necrosis. Compensatory mechanisms ultimately falter due to advancing venous stasis, abnormal drainage, and concomitant compromised arterial blood flow to the underlying brain [4,12,20]. The cumulative incidence curves **(Figure 3)** we created from our data demonstrate this as a notable disparity in the timeline of the appearance of vein abnormalities and the onset of calcifications.

The absence of cortical veins in SWS with resultant centripetal venous drainage into enlarged medullary veins or anomalous
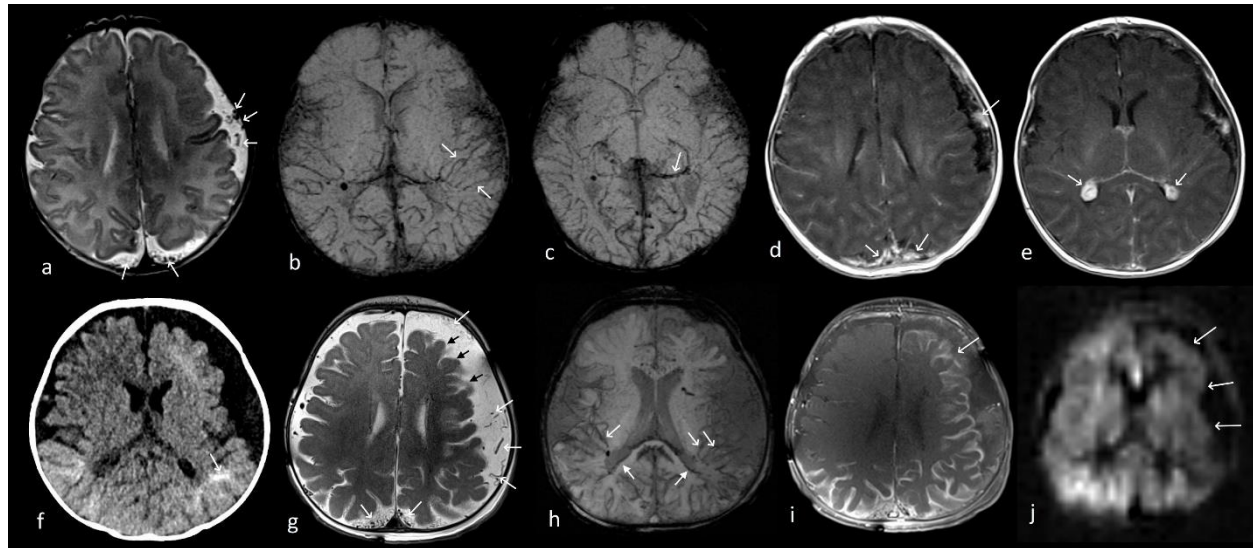

Figure 4. 11-day-old boy presenting with facial and chest port-wine stain.

(a-e) Initial MRI at 11 days of age showed extensive bilateral cerebral hemispheric involvement with the following signs: (a) Axial T2WI: subarachnoid varicose network (arrows) predominantly involving the left side; (b and c) Axial SWI MinIP shows prominence of the trans medullary veins (arrows in b) and deep extra ventricular veins (arrows in c) on the left; (d and e) Axial T1 TSE post-contrast shows enhancement of the subarachnoid varicose network (arrows in d), distant from the pial surface of the brain, which is not enhancing. The choroid plexus has a bulky appearance bilaterally (arrows in e).

(f) At 5 months of age, a CT was performed because of the onset of seizures: Axial non-contrast CT shows interval development of calcifications (arrow).

(g – j) Follow-up at 7 months of age demonstrates interval progression of brain involvement (atrophy) predominately on the left side: (g) Axial T2WI shows interval progression of the subarachnoid varicose network (white arrows) and cortical atrophy (black arrows); (h) Axial SWI MinIP shows progression of trans medullary veins (open arrows) and subependymal veins (closed arrows); (i) Axial T1 TSE post-contrast shows the interval development of bilateral abnormal pial enhancement coating the surface of the brain with outlining of the sulci and extending to the left frontal lobe (arrow); (j) ASL showing decreased perfusion on the left side, corresponding to the region of abnormal pial enhancement (arrows).

deep veins in SWS has been described previously [19,21,22]. It has been proposed that in SWS, the anomalous venous plexus over the cerebral surface (subarachnoid varicose network) results in abnormal cortical drainage, progressive venous stasis, and chronic hypoxia with secondary enlargement of trans medullary venous collaterals redirecting flow toward the deep venous system [16]. It has also been proposed that over time, the subarachnoid varicose network is exacerbated by progressive overburdening and possible occlusion of deep veins, with the resultant centrifugal rerouting of deep cerebral venous drainage into the already overburdened anomalous surface venous plexus (23). In this latter context, the subarachnoid varicose network represents dilated venous channels in the subarachnoid space attempting to divert venous blood away from the cortex towards the venous sinuses—a collateral pathway. Both scenarios explain why the subarachnoid varicose network is present at the early stages of the disease, around the

162   same time as various other dilated alternative drainage pathways that have been described in this study **(Figure 3 and Figure 4).**

163   Even though classic embryology does not completely explain the formation of the subarachnoid varicose network (also known

164   as pial angioma) in SWS [14], it is suggested that it results from failure of the primitive cerebral venous plexus to regress and properly

165   mature at 4–8 weeks of gestation, when deep medullary veins should become disconnected from the surface network [20,23]. A non-

166   thrombotic veno-occlusive process has been suggested as an underlying mechanism, which commences in utero and progresses

167   postnatally [21,23]. It is therefore understandable that brain changes have been reported as early as the prenatal period [24]. This would

168   also account for why certain patients exhibit overwhelmed compensation mechanisms as early as during the neonatal period **(Figure

169   5).**

170   It has been suggested that mutations occurring early in fetal development likely affect the brain, skin, and eyes, leading to the

171   full spectrum of SWS [25]. Global expression of p.R183Q GNAQ early during development is incompatible with survival [26], while

172   mutations occurring later in fetal life may have a limited impact and manifest as isolated Port Wine Stain. [25]. According to the

173   Roach scale (1992), SWS is classified into three types: Type I with both facial and leptomeningeal angiomas; and may have

174   glaucoma, Type II with facial angiomas alone and; may have glaucoma; and Type III with isolated leptomeningeal angiomas;

175   usually without glaucoma [27]. Based on this classification our cases fall into the Type I category (if our intracranial findings are

176   considered as equivalent of what is termed a leptomeningeal angioma). Additionally, all of our patients presented with high-risk

177   port wain stains (Online Supplemental Data). Hemifacial, forehead, and median port wine stain phenotypes involve skin originating

178   from the frontonasal placode, which shares common progenitor cells with the brain [28,29]; the severity of SWS is significantly higher

179   with these phenotypes. [11]. Bilaterality, V1 distribution, and extensive port wain stain with V2 and V3 involvement of the trigeminal

180   nerve also contribute to the risk of SWS [30,31]. Many authors have recommended early MRI scans (before 3 months of age) in

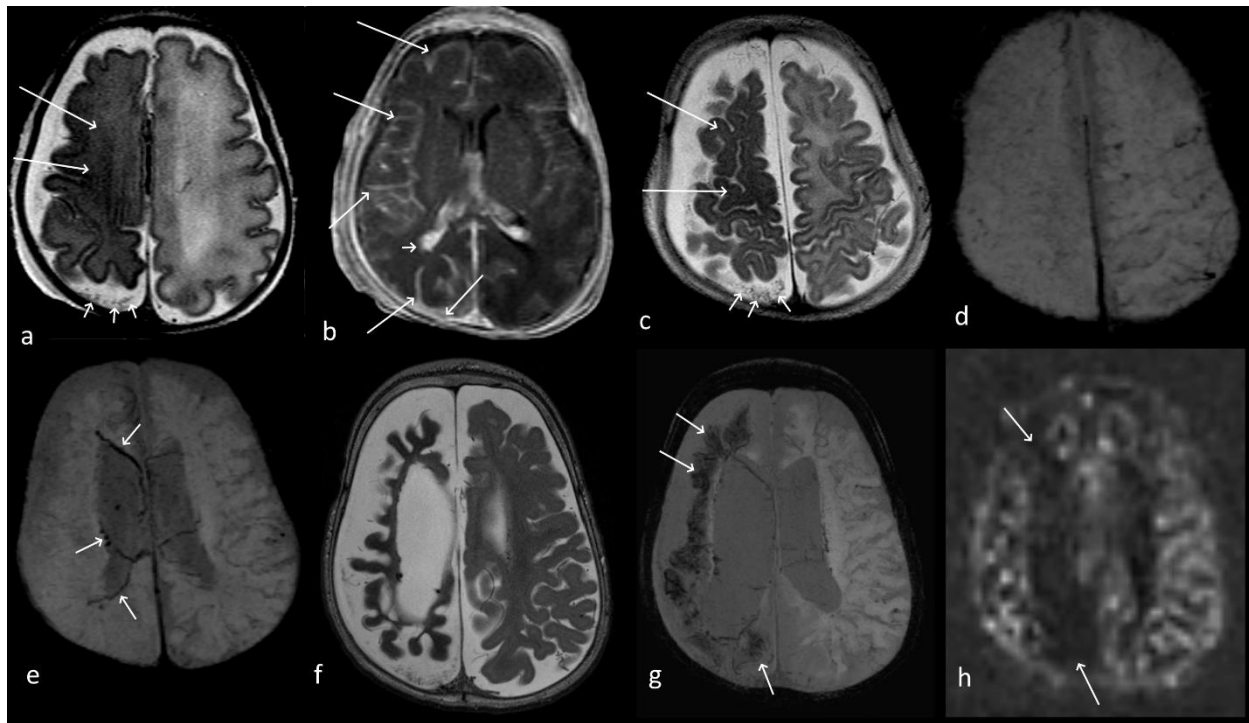181   patients presenting these clinical features [29,31,32].

Figure 5. 7-week-old girl born at 26 weeks' gestation showing clinically an erythematous rash on the right side of the face, left forehead, and right upper chest.

(a-b) Initial MRI at 7 months of age: (a) Axial T2WI shows atrophy of the right cerebral hemisphere with decreased T2 signal in the white matter ipsilaterally, in keeping with accelerated myelination (long arrows). Note the subarachnoid varicose network outlined by CSF, best seen posteriorly over the right parietal lobe (short arrows); (b) Axial post-contrast T1 TSE shows abnormal pial enhancement on the right, outlining the sulci (long arrows), as well as enlargement of the ipsilateral choroid plexus (short arrow).

(c-e) Follow-up at 3 months: (c) Axial T2WI shows the subarachnoid varicose network posteriorly to be more prominent (short arrows), as well as ongoing brain atrophy and signs of accelerated myelination (long arrows); (d and e) Axial SWI MinIP shows paucity of cortical veins on the right side as compared to the left, while there is prominence of the subependymal veins (arrows in e).

(f-h) Follow-up at 10 months of age: (f) Axial T2WI shows severe progression of right hemispheric atrophy; (g) SWI MinIP shows coarse susceptibility artifacts involving the right frontal and parietal lobe in keeping with calcifications (arrows); (h) ASL shows areas of decreased perfusion in the right hemisphere (arrows).

182   We have shown a variety of venous abnormalities representing dilated alternative drainage pathways to counter venous
183   hypertension, which builds over time as the result of the abnormal cortical venous drainage [3,21]. Using the k-means clustering, we
184   have shown using early MRI scans in our cohort, that the presence of a prominent subarachnoid varicose network, along with
185   enlargement of trans medullary veins, subependymal veins, and enlargement of the choroid plexus, precedes the enlargement of
186   deep extra ventricular veins, myelination changes, pial enhancement, atrophy, and calcifications (Online Supplemental Data).
187   Similar to ourselves, Juhász et al. described that the alternative collateral drainage for venous blood toward the deep cerebral venous
188   system becomes increasingly prominent, presumably as the cortical veins occlude progressively [2]. This explains why compensatory
189   vein dilatation is depicted first. Other studies have also demonstrated the evolution of compensatory venous pathways in SWS
190   using routine MR sequences [4,22]. Some authors have also described increased thickness of the choroid plexus as a sensitive and
191   specific sign to support the early diagnosis of SWS, when contrast MRI is not available or does not as yet show pial enhancement
192   [25]. Under the same pathophysiology, ineffective venous drainage leads to choroid plexus engorgement, supported by the frequent
193   observation of engorged ependymal veins (centripetal venous drainage). [33].
194   Understanding the primary issue—failure to develop cortical veins for proper drainage and subsequent venous hypertension —
195   helps explain why choroid plexus enlargement is a radiological sign of venous congestion from poor venous drainage. This same
196   underlying pathophysiology also accounts for the engorgement of the subarachnoid varicose network, which likely results from the
197   centrifugal rerouting of deep cerebral venous drainage.
198   In this study, we purposefully distinguished the presence of engorged vascular structures within the subarachnoid space from
199   abnormal post-contrast enhancement of the pia mater, and although not statistically significant (likely due to small number of
200   cases), this revealed noteworthy differences. The subarachnoid varicose network was identified as early as 5 days of age, with other
201   alternative venous pathways being detected by 11 days of age. In contrast, pial enhancement was observed earliest at 35 days of
202   life.
203   The presence of leptomeningeal or pial enhancement has traditionally been considered an essential diagnostic imaging sign of
204   SWS [7,12] and has been considered the radiologic representation of the so-called "pial angioma." However, in a recent study,
205   Venkatakrishna, et al. [34], evaluated histopathology specimens of 5 patients with SWS who underwent surgery, and demonstrated
206   that the subarachnoid varicose network is not a thickening or abnormality of the pia mater itself, but is observed separately within
207   the subarachnoid space as a network of varying-sized venous structures with flow-voids. These were presumed to represent an
208   alternative venous drainage pathway to compensate for the maldevelopment of cortical veins, which is the primary abnormality in
209   SWS.
210   Although pial enhancement has been reported as an early sign seen in the diagnosis of pre-symptomatic patients younger than
211   3 months of age [12], we found that pial enhancement itself is not as frequently present in the very early stages and although it can
212   be seen within the first 2 months. It is preceded by the appearance of various venous drainage compensatory pathways, primarily
213   the subarachnoid varicose network, which is frequently present. Venous drainage compensatory pathways were identified using
214   MinIP SWI sequence, because of its sensitivity for venous structures, and on T2-weighted imaging, in which the subarachnoid
215   varicose network stands out as flow voids (dark) against the background subarachnoid cerebrospinal fluid (bright) [22].
216   We also demonstrated that post-contrast enhancement of the subarachnoid varicose network is independent from the post-
217   contrast enhancement of the pia mater, with the latter occurring later in the disease progression. In this way, we determined that
218   the alternative venous drainage pathways preceded that of the typical pial enhancement, both of which are seen with contrast-
219   enhanced spin echo T1 and contrast-enhanced 3D MPRAGE [12,16].
220   There is also increasing evidence that suggests leptomeningeal or pial-arachnoid enhancement is linked to cortical gray matter
221   tissue loss rather than an angioma [35]. Given that gray matter tissue loss develops gradually over time in these patients, it is
222   understandable why atrophy and any pial or pial-arachnoid enhancement related to this atrophy may not be reliable early diagnostic
223   features for SWS. Likewise, hypermyelination has been associated with transient hyperperfusion and hypermetabolism in the
224   affected area, believed to be a response to stress (hypoxia) [20], thus typically manifesting as a consequent/subsequent finding.
225   Similar to other researchers [29,32] we advocate for protocols that incorporate early imaging before 3 months of age for patients
226   with high-risk port wine stains. We suggest including at least T2 and MinIP SWI sequences, to identify the alternative venous
227   pathways as an early sign of brain involvement in SWS, particularly recognizing the subarachnoid varicose network as a different
228   entity from pial enhancement, the former which can be visualized even without post-contrast enhancement.
229   Potential benefit of pre-symptomatic antiepileptic treatment combined with aspirin has been proposed [36], but no prospective
230   studies have been completed. Some children with high risk for seizures may benefit from pre-symptomatic treatment, for example
231   when bilateral SWS is suspected in the presence of extensive bilateral port wine stains [37]. Although the use of aspirin in this small
232   series did not prevent seizures, the mortality rate in these patients is zero, and seizures have been controlled medically in the
233   majority (Online Supplemental Data). Other studies acknowledge the role of the endothelial Gαq-R183Q gene and specific
234   antiangiogenic therapies (including anti PI3K or MAPK) for further research and drug development particularly in the management
235   of Port-Wine stains [38,39]. However, these have not been evaluated in the prevention of cerebral injury and seizures.
236   Our study has several limitations. The number of patients was limited by the low prevalence of the disease and the strict inclusion

237 criteria of having at least 2 available MRIs before the age of 2 with a gap of at least 2 months between scans.

238   The lack of universal consensus on the appropriate age for conducting MRI surveillance in children with SWS presented a
239 challenge for the retrospective collection of data with regard to age at which scanning was performed. K-means clustering relies
240 on the number of patients and the variables provided, and our sample was limited to 9 patients, underscoring the need for a multi-
241 institutional study. When dealing with small sample sizes, obtaining reliable clustering results can be challenging and result in
242 unstable clustering outcomes, poor results, and low efficiency [40]. The main idea of this analysis in our paper was to show how
243 clustering analysis can help in studying this evolving disease and provide a template for evaluating larger patient cohorts.
244 Additionally, our clustering analysis only used prevalence data at specific time points; adding more variables or changing the time
245 points could potentially influence the results. To create the cumulative incidence curves, the start point is the day of birth, and we
246 assumed that the prevalence of all lesions at birth is zero. However, given that SWS is a congenital condition, it is possible that
247 these lesions may have been present during the fetal period, which can potentially influence the baseline prevalence. Additionally,
248 determining the precise date of lesion emergence requires repeated MRIs, which is not feasible. As a result, in the cumulative
249 incidence curve, if a patient had a lesion on an MRI, we took the date of the MRI as the initial day of lesion emergence. Lastly, a
250 selection bias for the most severe patients with high-risk port wine stains is unavoidable in this retrospective study as this disease
251 is suspected on clinical grounds and imaging requests are triggered from these, with the most severe patients presenting at earlier
252 ages.

CONCLUSIONS

254 Dilated venous channels develop early on as a compensation mechanism for absent or thrombosed cortical veins and pre-date the
255 traditional findings associated with SWS, such as atrophy and calcification, which result later and reflect established brain necrosis.
256 Dilated venous channels also pre-date the appearance of abnormal contrast enhancement of the pia, which has been previously
257 referred to as a "pial angioma." In this regard, we have demonstrated clear differences in timing between the appearance of a
258 subarachnoid vascular network (seen on both T2 and with SWI) and the appearance of pial enhancement. MRI in children with
259 SWS should be used to detect centripetal venous collateral pathways and centrifugal collateral pathways in the form of an engorged
260 subarachnoid varicose network very early in post-natal life, early enough to allow for interventions to prevent brain necrosis.

This preprint represents the accepted version of the article and also includes the supplemental material; it differs from the printed version of the article.

REFERENCES

1.   1.   Vellieux G, Frazzini V, Pichit P, et al. A review of the natural history of Sturge-Weber syndrome through adulthood. J Neurol 2022;269:4872–83. DOI: https://10.1007/s00415-022-11132-9

2.   2.   Juhász C, Haacke EM, Hu J, et al. Multimodality imaging of cortical and white matter abnormalities in Sturge-Weber syndrome. AJNR Am J Neuroradiol 2007;28:900–6.

3.   3.   Sarma A, Martin D, Pruthi S, et al. Imaging the cerebral veins in pediatric patients: beyond dural venous sinus thrombosis. Radiographics 2023;43:e220129. DOI: https://10.1148/rg.220129

4.   4.   Clifford SM, Ghosh A, Zandifar A, et al. Arterial spin-labeled (ASL) perfusion in children with Sturge-Weber syndrome: a retrospective cross-sectional study. Neuroradiology 2023;65:1825–34. DOI: https://10.1007/s00234-023-03224-8

5.   5.   Comi AM. Sturge-Weber syndrome. Handb Clin Neurol 2015;132:157–68. DOI: https://10.1016/B978-0-444-62702-5.00011-1

6.   6.   Vedmurthy P, Pinto ALR, Lin DDM, et al. Study protocol: retrospectively mining multisite clinical data to presymptomatically predict seizure onset for individual patients with Sturge-Weber. BMJ Open 2022;12:e053103. DOI: https://10.1136/bmjopen-2021-053103

7.   7.   Sudarsanam A, Ardern-Holmes SL. Sturge-Weber syndrome: from the past to the present. Eur J Paediatr Neurol 2014;18:257–66. DOI: https://10.1016/j.ejpn.2013.10.003

8.   8.   Miao Y, Juhász C, Wu J, et al. Clinical correlates of white matter blood flow perfusion changes in Sturge-Weber syndrome: a dynamic MR perfusion-weighted imaging study. AJNR Am J Neuroradiol 2011;32:1280–5. DOI: https://10.3174/ajnr.A2540

9.   9.   Lin DDM, Barker PB, Kraut MA, et al. Early characteristics of Sturge-Weber syndrome shown by perfusion MR imaging and proton MR spectroscopic imaging. AJNR Am J Neuroradiol 2003;24:1912–5.

10.   10.   Pouliquen G, Fillon L, Dangouloff-Ros V, et al. Arterial Spin-Labeling Perfusion Imaging in the Early Stage of Sturge-Weber Syndrome. AJNR Am J Neuroradiol 2022;43:1516–22. DOI: https://10.3174/ajnr.A7643

11.   11.   Zallmann M, Mackay MT, Leventer RJ, et al. Retrospective review of screening for Sturge-Weber syndrome with brain magnetic resonance imaging and electroencephalography in infants with high-risk port-wine stains. Pediatr Dermatol 2018;35:575–81. DOI: https://10.1111/pde.13598

12.   12.   Bar C, Pedespan J-M, Boccara O, et al. Early magnetic resonance imaging to detect presymptomatic leptomeningeal angioma in children with suspected Sturge-Weber syndrome. Dev Med Child Neurol 2020;62:227–33. DOI: https://10.1111/dmcn.14253

13.   13.   Pearl M, Gregg L, Gandhi D. Cerebral venous development in relation to developmental venous anomalies and Vein of Galen aneurysmal malformations. Semin Ultrasound CT MR 2011;32:252–63. DOI: https://10.1053/j.sult.2011.02.001

14.   14.   Raybaud C. Normal and abnormal embryology and development of the intracranial vascular system. Neurosurg Clin N Am 2010;21:399–426. DOI: https://10.1016/j.nec.2010.03.011

15.   15.   Lai LM, Sato TS, Kandemirli SG, et al. Neuroimaging of neonatal stroke: venous focus. Radiographics 2024;44:e230117. DOI: https://10.1148/rg.230117

16.   16.   Hu J, Yu Y, Juhasz C, et al. MR susceptibility weighted imaging (SWI) complements conventional contrast enhanced T1 weighted MRI in characterizing brain abnormalities of Sturge-Weber Syndrome. J Magn Reson Imaging 2008;28:300–7. DOI: https://10.1002/jmri.21435

17.   17.   Parsa CF. Sturge-weber syndrome: a unified pathophysiologic mechanism. Curr Treat Options Neurol 2008;10:47–54. DOI: https://10.1007/s11940-008-0006-0

18.   18.   Pedregosa F, Varoquaux G, Gramfort A, et al. Scikit-learn: Machine Learning in Python. Journal of Machine Learning Research 2011. . [Epub ahead of print].

19.   19.   Mentzel H-J, Dieckmann A, Fitzek C, et al. Early diagnosis of cerebral involvement in Sturge-Weber syndrome using high-resolution BOLD MR venography. Pediatr Radiol 2005;35:85–90. DOI: https://10.1007/s00247-004-1333-2

20.   20.   Moritani T, Kim J, Sato Y, et al. Abnormal hypermyelination in a neonate with Sturge-Weber syndrome demonstrated on diffusion-tensor imaging. J Magn Reson Imaging 2008;27:617–20. DOI: https://10.1002/jmri.21248

21.   21.   Curé JK, Holden KR, Van Tassel P. Progressive venous occlusion in a neonate with Sturge-Weber syndrome: demonstration with MR venography. AJNR Am J Neuroradiol 1995;16:1539–42.

22.   22.   Mandelstam S, Andronikou S. MRI evaluation of venous abnormalities in children with Sturge-Weber syndrome. J Pediatr Neurol 2004;02:029–32. DOI: https://10.1055/s-0035-1557187

23.   23.   Raets M, Dudink J, Raybaud C, et al. Brain vein disorders in newborn infants. Dev Med Child Neurol 2015;57:229–40. DOI: https://10.1111/dmcn.12579

24.   24.   Cagneaux M, Paoli V, Blanchard G, et al. Pre- and postnatal imaging of early cerebral damage in Sturge-Weber syndrome. Pediatr Radiol 2013;43:1536–9. DOI: https://10.1007/s00247-013-2743-9

25.   25.   Catsman-Berrevoets CE, Koudijs SM, Buijze MSJ, et al. Early MRI diagnosis of Sturge Weber Syndrome type 1 in infants. Eur J Paediatr Neurol 2022;38:66–72. DOI: https://10.1016/j.ejpn.2022.04.002

26.   26.   Wetzel-Strong SE, Galeffi F, Benavides C, et al. Developmental expression of the Sturge-Weber syndrome-associated genetic mutation in Gnaq: a formal test of Happle's paradominant inheritance hypothesis. Genetics 2023;224. DOI: https://10.1093/genetics/iyad077

27.   27.   Roach ES. Neurocutaneous syndromes. Pediatr Clin North Am 1992;39:591–620. DOI: https://10.1016/S0031-3955(16)38367-5

28.   28.   Dutkiewicz A-S, Ezzedine K, Mazereeuw-Hautier J, et al. A prospective study of risk for Sturge-Weber syndrome in children with upper facial port-wine stain. J Am Acad Dermatol 2015;72:473–80. DOI: https://10.1016/j.jaad.2014.11.009

29.   29.   Waelchli R, Aylett SE, Robinson K, et al. New vascular classification of port-wine stains: improving prediction of Sturge-Weber risk. Br J Dermatol 2014;171:861–7. DOI: https://10.1111/bjd.13203

30.   30.   Mehta M, Salas AH, Fay A. Trigeminal dermatome distribution in patients with glaucoma and facial port wine stain. Dermatology (Basel) 2009;219:219–24. DOI: https://10.1159/000235546

31.   31.   Sánchez-Espino LF, Ivars M, Antoñanzas J, et al. Sturge-Weber Syndrome: A Review of Pathophysiology, Genetics, Clinical Features, and Current Management Approache. Appl Clin Genet 2023;16:63–81. DOI: https://10.2147/TACG.S363685

32.   32.   Mankel FL, Papandreou A, Mankad K, et al. Diagnostic pathway and management of first seizures in infants with Sturge-Weber syndrome. Dev Med Child Neurol https://doi.org/10.1111/dmcn.15983. DOI: https://10.1111/dmcn.15983

33.   33.   Madhukar M, Choudhary AK, Boal DK, et al. Choroid plexus: normal size criteria on neuroimaging. Surg Radiol Anat 2012;34:887–95. DOI: https://10.1007/s00276-012-0980-5

9

34. 34. Venkatakrishna SSB, Viaene AN, Cerron-Vela CR, et al. Radio-pathologic correlation: no pial angioma-subarachnoid varicose network drainage pathway in Sturge-Weber syndrome. Childs Nerv Syst https://doi.org/10.1007/s00381-024-06490-w. DOI: https://10.1007/s00381-024-06490-w

35. 35. Bergsland N, Ramasamy D, Tavazzi E, et al. Leptomeningeal Contrast Enhancement Is Related to Focal Cortical Thinning in Relapsing-Remitting Multiple Sclerosis: A Cross-Sectional MRI Study. AJNR Am J Neuroradiol 2019;40:620–5. DOI: https://10.3174/ajnr.A6011

36. 36. Day AM, Hammill AM, Juhász C, et al. Hypothesis: Presymptomatic treatment of Sturge-Weber Syndrome With Aspirin and Antiepileptic Drugs May Delay Seizure Onset. Pediatr Neurol 2019;90:8–12. DOI: https://10.1016/j.pediatrneurol.2018.04.009

37. 37. Sabeti S, Ball KL, Bhattacharya SK, et al. Consensus Statement for the Management and Treatment of Sturge-Weber Syndrome: Neurology, Neuroimaging, and Ophthalmology Recommendations. Pediatr Neurol 2021;121:59–66. DOI: https://10.1016/j.pediatrneurol.2021.04.013

38. 38. Nguyen V, Hochman M, Mihm MC, et al. The Pathogenesis of Port Wine Stain and Sturge Weber Syndrome: Complex Interactions between Genetic Alterations and Aberrant MAPK and PI3K Activation. Int J Mol Sci 2019;20. DOI: https://10.3390/ijms20092243

39. 39. Huang L, Bichsel C, Norris AL, et al. Endothelial GNAQ p.R183Q Increases ANGPT2 (Angiopoietin-2) and Drives Formation of Enlarged Blood Vessels. Arterioscler Thromb Vasc Biol 2022;42:e27–43. DOI: https://10.1161/ATVBAHA.121.316651

40. 40. Zhu H. Constructing an enterprise management system using an improved clustering algorithm. Mobile Information Systems 2022;2022:1–9. DOI: https://10.1155/2022/9119452
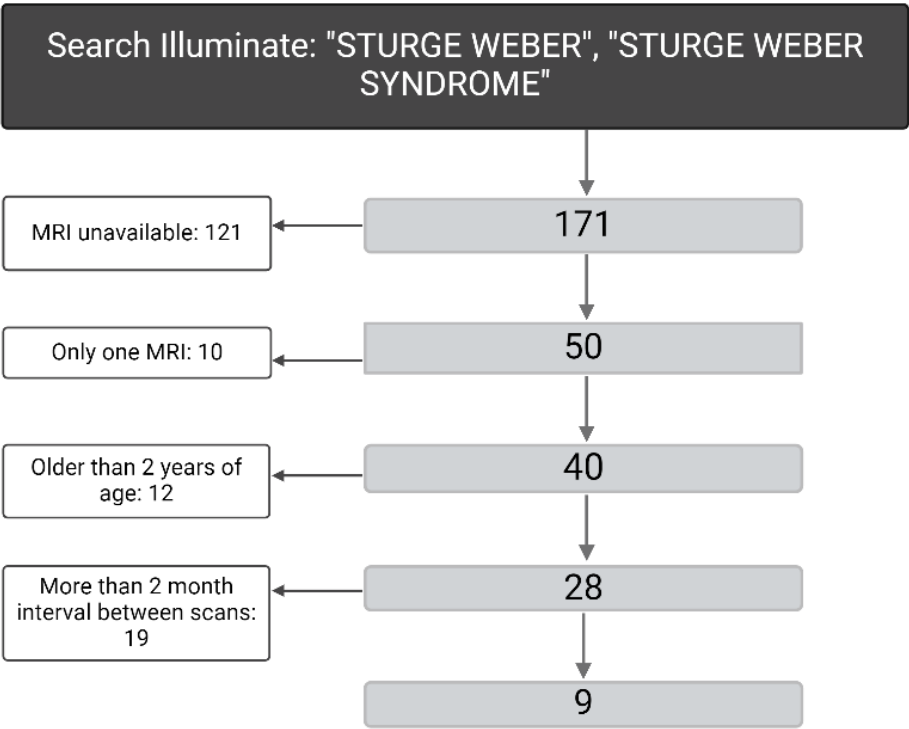
Online Figure 1. Flow diagram showing the inclusion and exclusion criteria and resultant study population.
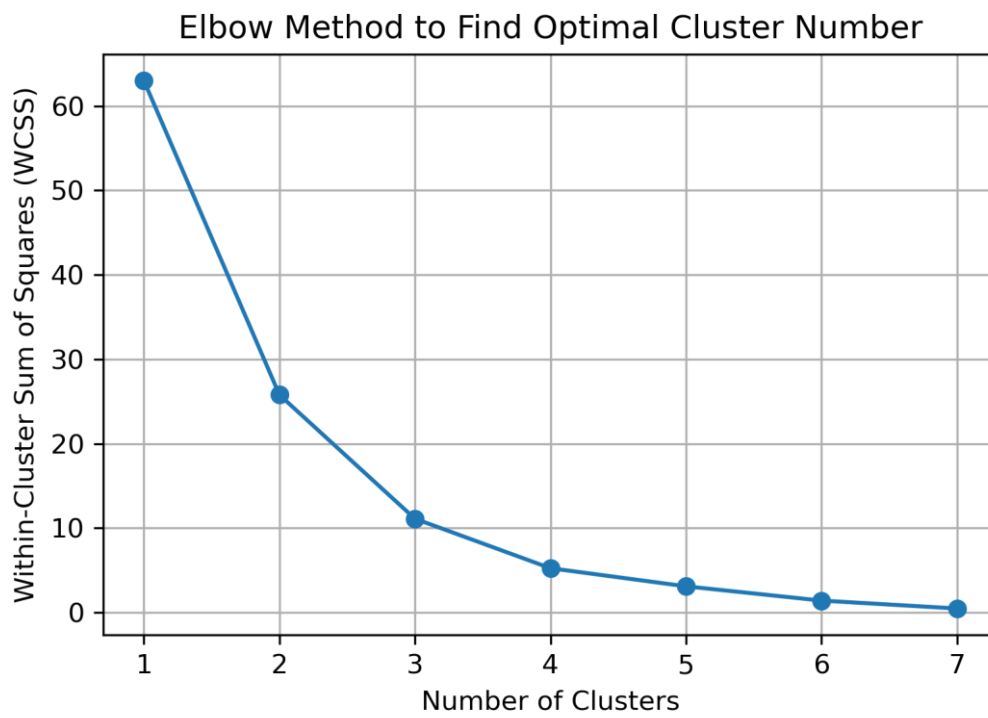
Online Figure 2. Elbow plot showing the within-cluster sum of squares (WCSS) as a function of the number of clusters.
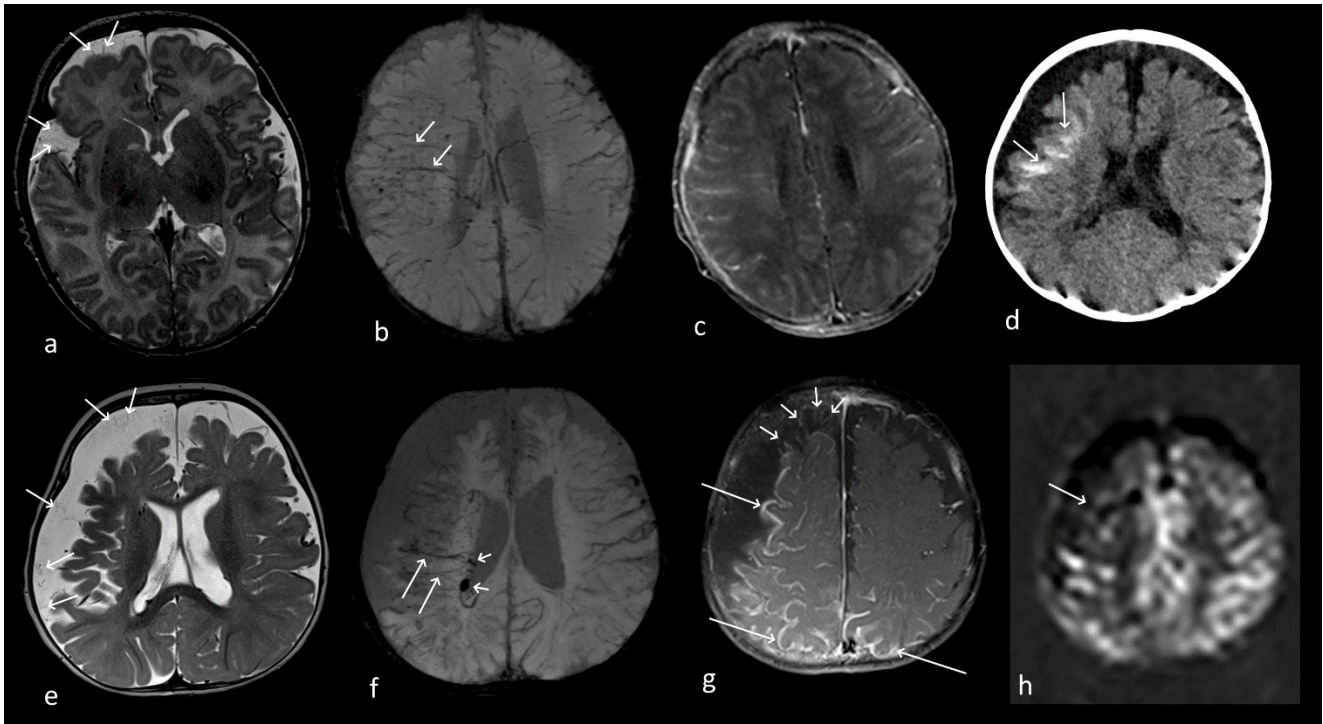
Online Figure 3. A 5-week-old girl with a port wine stain on right side in the V1, V2, and V3 distribution.

(a-c) Initial MRI at 5 weeks of age: (a) Axial T2WI shows presence of a subarachnoid varicose network around the right frontal, parietal, and temporal lobes (arrows). (b) Axial SWI MinIP shows prominence of the trans medullary veins in the right fronto-parietal lobes (arrows) but no calcification. (c) T1 TSE post-contrast shows enhancement of the subarachnoid vascular network but no clear abnormal pial enhancement extending over the cerebral surface into the sulci.

(d) CT was performed at 5 months due to the onset of seizures: Axial CT shows interval development of significant right hemispheric atrophy and subcortical coarse calcifications (arrows).

(e-h) Follow-up at 9 months of age: (e) Axial T2WI shows ongoing atrophy and a fine network of serpiginous vessels occupying the expanded CSF space, comprising the enlarging subarachnoid varicose network (arrows); (f) Axial SWI MinIP shows ongoing prominence of the trans medullary (long arrows) and subependymal veins (short arrows). (g) Axial T1 TSE-post contrast shows pial enhancement lining the brain surface and sulci, which extends to the contralateral side (long arrows) and is seen separately from enhancement of the subarachnoid varicose network (short arrows); (h) Axial ASL perfusion shows decreased perfusion in the right frontal lobe (arrow).

Online Table 1. Evolving MRI findings in the first 2 years of life in children with Sturge Weber Syndrome

Case	1st MRI										2nd MRI										3rd MRI									
	Age (days)	SVN	Trans medullary veins	Subependymal veins	Deep-extraventricular veins	Choroid plexus enlargement	Pial-arachnoid enhancement	Accelerated myelination	Atrophy	Calcifications	Age (days)	SVN	Trans medullary veins	Subependymal veins	Deep-extraventricular veins	Choroid plexus enlargement	Pial-arachnoid enhancement	Accelerated myelination	Atrophy	Calcifications	Age (days)	SVN	Trans medullary veins	Subependymal veins	Deep-extraventricular veins	Choroid plexus enlargement	Pial-arachnoid enhancement	Accelerated myelination	Atrophy	Calcifications
1	35	✓	✓	✓	✓	✓	✓	✓	✓	×	181	✓	✓	✓	✓	✓	✓	✓	✓	×	294	✓	✓	✓	✓	✓	✓	✓	✓	✓
2	22	✓	✓	✓	✓	×	×	×	×	×	97	✓	✓	✓	✓	×	✓	✓	✓	×	Not performed									
3	217	✓	✓	✓	✓	✓	✓	✓	✓	×	465	✓	✓	✓	✓	✓	✓	×	✓	✓	Not performed									
4	11	✓	✓	✓	✓	✓	×	×	×	×	174	✓	✓	✓	✓	✓	✓	✓	✓	×	261	✓	n/a	✓	✓	n/a	n/a	✓	✓	n/a
5	180	✓	✓	✓	✓	×	✓	×	×	×	492	✓	✓	✓	✓	✓	✓	×	✓	×	Not performed									
6	123	✓	✓	×	✓	×	✓	✓	✓	×	717	✓	✓	×	✓	✓	✓	✓	✓	✓	Not performed									
7	53	✓	✓	✓	×	✓	✓	✓	✓	×	119	✓	✓	✓	✓	✓	✓	✓	✓	×	325	✓	✓	✓	✓	✓	✓	n/a	✓	✓
8	5	✓	×	×	×	✓	×	×	×	×	97	✓	×	×	×	✓	✓	×	×	×	208	✓	n/a	✓	✓	✓	✓	✓	✓	n/a
9	6	×	×	×	×	✓	×	×	×	×	192	×	✓	✓	✓	✓	✓	✓	✓	×	Not performed									

SVN, Subarachnoid Varicose network; n/a Not available (required sequence not performed)

Online Table 2: Clinical findings in patients with SWS.

Case	Sex	1st MRI					2nd MRI				3rd MRI				Surgery **	Seizure free	Developmental delay
		Age	Clinical Signs	Symptoms	Associated diagnosis	Rx.	Age	Symptoms	Associated diagnosis	Rx.	Age	Symptoms	Associated diagnosis	Rx			
1	F	35	Port Wine Stain V1-V3 distribution, eye glaucoma and choroidal angioma	Pre-symptomatic	none	Aspirin	181	Focal seizure (left side) progressed to tonic-clonic seizures, with postictal Todd's paralysis	none	Oxcarbazepine, fosphenytoin, aspirin	294	Seizure-free	none	Same	no	yes	no
2	F	22	Port wine stain, V1 distribution	Pre-symptomatic	none	Aspirin	97	Focal seizure (left side) progressed to tonic-clonic seizures and status epilepticus	none	Keppra, aspirin					yes	yes	yes (motor)
3	M	217	Port Wine stain, V1-V2 distribution, eye glaucoma	Focal seizure (left side)	Active viral infection and fever	Keppra, aspirin	465	Focal seizure (left side) progressed to tonic-clonic seizures and left hemiparesis	none	Keppra, phenobarbital, aspirin					no	yes	no
4	M	11	Port Wine stain in bilateral V1-V2 distribution and left upper chest and arm and bilateral glaucoma	Pre-symptomatic	Tetralogy of Fallot, hemihypertrophy of the left arm	None	174	Focal seizure (left side)	Klippel-Trenaunay-Weber syndrome.	Trileptal, aspirin	261	Seizures with lethargy and decreased right-sided motor function	none	aspirin, oxcarbazepine and clobazam	Unknown*	Unknown*	Unknown*
5	M	180	Port Wine stain right V1-V2 and spotty in the V3 distribution and left V2 distribution. Right shoulder, arm, forearm hand in radial distribution, right leg, extending to sole, left lower	Focal seizures (left side)	none	Keppra, aspirin	492	Increased seizure activity	right monoparesis	Keppra, aspirin					no	yes	no

			leg, part of sole, right side of back, sacral area, some scattered areas in perineal area.													
6	F	123	Port Wine Stain V2 distribution	Focal seizures (left side)	Twin. Peripheral pulmonary stenosis.	Aspirin, keppra, vigabatrin, topamax	717	Seizure-free	none	Bicitra, topamax				no	yes	yes
7	F	53	Port-wine stain face, chest, right arm, right leg. Bilateral glaucoma	Pre-symptomatic	Born 26 weeks, Klippel Trenaunay, hypoplastic right jugular vein, duplicated SVC. Retinopathy of prematurity of both eyes, extensive Mongolian spots on right arm and trunk.	Aspirin	119	Infantile spams (left sife)	none	prednisolone	325	Infantile spasms with left-sided hypsarrhythmia	none	prednisolone, zonisamide	no	no	yes
8	M	5	Port-wine stains bilateral, bilateral glaucoma	Pre-symptomatic	Perinatal ischemic stroke	None	97	multiple seizures types, developmental delayed	none	aspirin, phenobarbital	208	Generalized tonic seizures	none	phenobarbital, trileptal, topamax	no	no	yes
9	M	6	Port wine stain, bilateral forehead areas, and CNV1-3 on the right side. Right glaucoma	Pre-symptomatic	none	none	192	Pre-symptomatic	none	aspirin				no	yes	no

Rx. Prescription

*Patient returned to his birth country

**Hemispherectomy